Journal of Power Sources 204 (2012) 116–121

Contents lists available at SciVerse ScienceDirect

Journal of Power Sources

journal homepage: www.elsevier.com/locate/jpowsour

Short communication

Hydrazine/air direct-liquid fuel cell based on nanostructured copper anodes

Eran Granot[a,1], Boris Filanovsky[a,1], Igor Presman[b], Iliya Kuras[b], Fernando Patolsky[a,*]

[a] School of Chemistry, the Raymond and Beverly Sackler Faculty of Exact Sciences, Tel-Aviv University, Tel-Aviv 69978, Israel
[b] Nanergy, Ltd., Hertzeliya, Israel

ARTICLE INFO

Article history:
Received 11 May 2011
Received in revised form 29 July 2011
Accepted 6 December 2011
Available online 13 December 2011

Keywords:
Fuel cell
Copper
Hydrazine
Anode
Nanotechnology
Nanostructures

ABSTRACT

Fuel cells (FCs) are promising electrochemical devices that convert the chemical energy of fuels directly into electrical energy, as long as the fuel is supplied.

This paper describes a room-temperature hydrazine/air direct-liquid fuel cell (DLFC) based on the use of *nanostructured* copper electrodes. We show that *nanostructured* copper electrodes function as highly efficient and ultra-long-lasting catalyst for the electro-oxidation of hydrazine. Our Cu/hydrazine anodes show high electrical efficiency for long periods of continuous operation (more than 500 h).

A hydrazine/air fuel cell prototype was built with a *nanostructured* Cu/hydrazine anode, combined with a commercial air cathode. The output of this cell is about 0.45 W at 1 A (0.1 A cm^{-2} corresponds to the anode area), and supplies about 2.3 Wh and 1300 Wh kg^{-1} hydrazine. The hydrazine discharge efficiency is higher than 85%.

1. Introduction

A fuel cell (FC) is a well-known electrochemical device that enables the conversion of the chemical energy of fuels directly into electrical energy, as long as the fuel is supplied. Fuel cells are characterized by high energy density (typically 2–8 kWh kg^{-1}), more than 10 times that of conventional batteries [1].

Several types of fuel cells have been developed over the last four decades [1–7]. However, as a result of many practical limitations, these fuel cells are still far from mass production. Only one type of room-temperature (RT) fuel cell has been used for space and military applications: a proton-exchange-membrane fuel cell (PEM-FC), that utilizes hydrogen under high pressure as fuel and pure oxygen [8].

Some of the most handicapping limitations of current fuel-cell technologies are related to the limited structural and functional stability of expensive noble-metal catalysts, like platinum and the platinum-group metals [1,4,16–21]. These are easily poisoned by different chemical species such as carbon monoxide, at even very low concentrations of a few ppm, and this inherently limits the operation of the fuel cell. Thus, finding low-cost efficient and stable catalysts is an essential requirement.

Copper, owing to its high conductivity and low cost, is extremely attractive as a catalyst for fuel-cell devices. However, copper has never been successfully applied for this purpose [9].

During the last decade, much research efforts have been focused on hydrogen-rich fuels, like methanol [13–15], sodium borohydride [1,16–21], ammonia-borane [22–26] and hydrazine [27].

Hydrazine is a low cost material and its synthesis is relatively simple. The basic source of hydrazine in nature (nitrogen and hydrogen) is unlimited and there is no recycling limitation. Hydrazine synthesis can be combined with the mass-production of ammonia. In addition, the decomposition products of hydrazine (nitrogen and water) are ecological friendly. Hydrazine, in its pure form (N_2H_4), is considered a hazardous compound, although less hazardous as the monohydrate ($N_2H_4{\cdot}H_2O$). However, hydrazine is non-explosive and is less toxic in dilute aqueous solutions. Moreover, several hydrazine salts have been reported as prospective anticancer drugs [28].

The electrochemical-oxidation of hydrazine in alkaline solution produces four electrons, nitrogen gas and water (1). The standard potential of hydrazine oxidation corresponds to −1.21 V, its theoretical specific electrical capacity is 3.35 Ah g^{-1}. The theoretical energy of a hydrazine/air fuel cell is 5.36 Wh g^{-1}.

$$NH_2{-}NH_2 + 4(OH)^- \rightarrow N_2 + 4H_2O + 4e^- \quad (1)$$

The first hydrazine fuel cell was developed more than forty years ago [29], but it has attracted renewed interest in recent years [30–34], mainly due to the increased cost of oil and growing demand for stationary and mobile applications, including vehicles.

* Corresponding author. Tel.: +972 3 6408327; fax: +972 3 6409293.
E-mail address: fernando@post.tau.ac.il (F. Patolsky).
[1] These authors contributed equally.

0378-7753/$ – see front matter © 2011 Elsevier B.V. All rights reserved.
doi:10.1016/j.jpowsour.2011.12.008

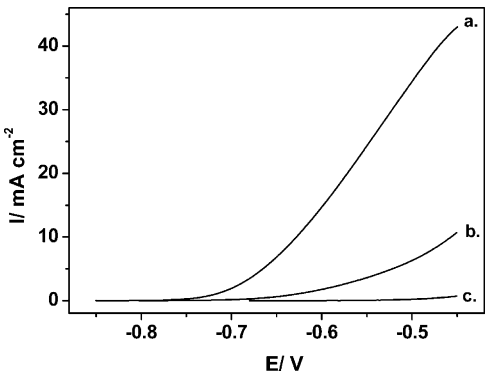

Fig. 1. The electro-oxidation of hydrazine with the use of different bare polished electrodes: (a) Cu, (b) Au and (c) Ag. Surface area of each electrode is 0.5 cm^2. The experiments were carried out in 0.4 M hydrazine, 1 M KOH, scan rate 50 mV s^{-1}. Ag/AgCl (sat. KCl) was used as the reference electrode.

The electrochemical properties of hydrazine in alkaline solutions have been studied over the last three decades [35–38]. Asazawa et al. [37] studied the electro-oxidation of hydrazine (and hydrazine derivatives) with the use of various metals such as nickel, cobalt, iron, copper and gold, and found that nickel and cobalt show the highest catalytic activity. However, in that study, copper was found not to be a good catalyst for the electro-oxidation of hydrazine, probably because the electrode structure was not adapted to hydrazine oxidation. Later, Asazawa et al. [33] used nickel and cobalt as catalysts for the development of a hydrazine/oxygen fuel cell, with the use of an anion-exchange membrane. The performance of this fuel cell is comparable to that of the hydrogen/polymer-electrolyte fuel cell (PEFC), and exceeds that of the direct methanol fuel cell (DMFC), but requires a continuous supply of pure oxygen. Li et al. [35] found that Pd/Ni (on a carbon-nanotube support) is an effective catalyst for the electro-oxidation of hydrazine. This study also showed that nickel provides catalytic activity for the electro-oxidation of hydrazine only at high temperatures (80 °C).

Recently, different catalysts were also applied for the development of hydrazine sensors [10,39,40]. The electrochemical oxidation of hydrazine occurs in the anodic potential range of 0.2–0.7 V (vs. Ag/AgCl) in these systems. Karim-Nezhad et al. [10] developed a copper (hydr)oxide-modified carbon electrode characterized by improved stability toward corrosion and improved electrochemical performance; the hydrazine-oxidation peak appears at about 0.3 V (vs. Ag/AgCl), probably because this electrode is coated by a film of CuO. The copper (hydr)oxide electrode cannot be used as a catalyst for hydrazine fuel cells since the hydrazine peak potential is out of range; the anodic potential must be lower than −0.7 V (vs. Ag/AgCl) for fuel-cell applications.

However, Cu^{2+} species produce high catalytic activity for homogeneous hydrazine oxidation [41,42]. In another publication it was shown that the hydrazine-oxidation reaction could become faster by seven orders of magnitude in the presence of a Cu^{2+}-complex catalyst [43].

The critical question is whether the electrochemical oxidation of hydrazine can be also catalyzed by the Cu/Cu(II) couple. The contradiction between these reports, describing high or low activity of the Cu/Cu^{n+} system toward the electro-oxidation of hydrazine, required us to investigate the electro-oxidation of hydrazine with the use of a copper catalyst. We will show that Cu/hydrazine or *nanostructured*-Cu/hydrazine anodes may be used effectively in the development of low-cost hydrazine/air fuel cells.

The purpose of this work was the development of a new *nanostructured*-Cu/hydrazine-based RT fuel cell. This development followed our previous results regarding the electro-oxidation of

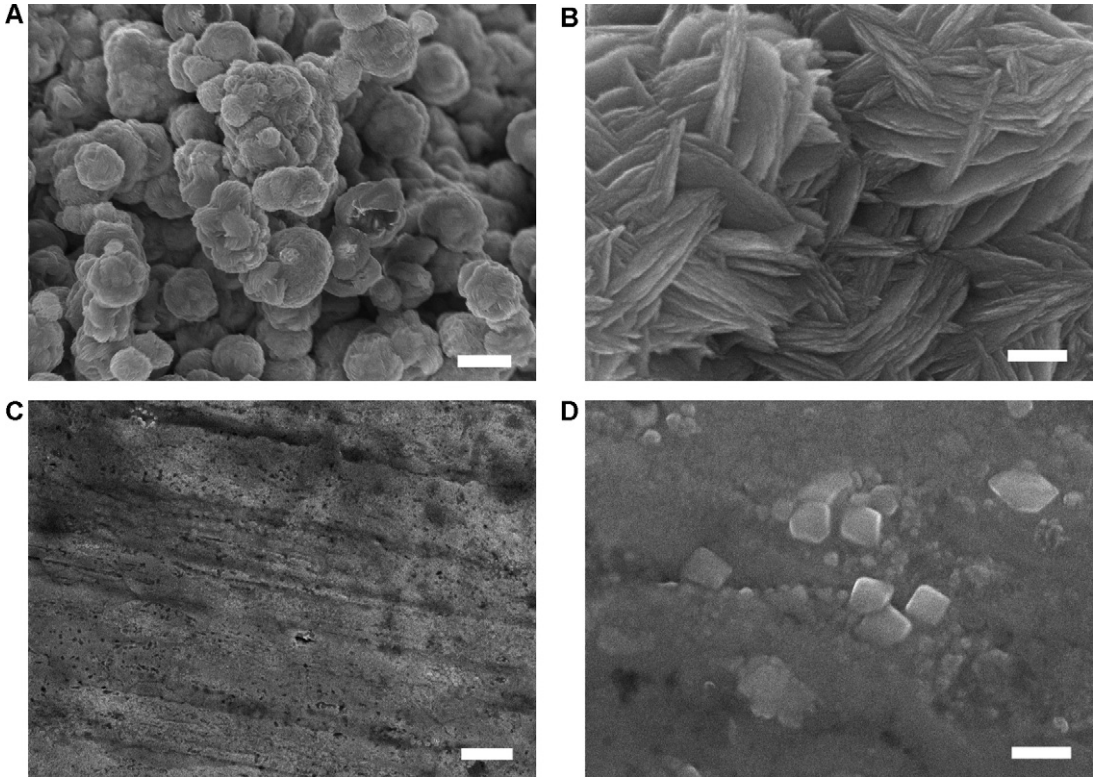

Fig. 2. Representative HRSEM images: (A) and (B) *nanotextured* woven-Cu electrodes, (C) and (D) conventional woven-Cu electrode. Scale bars for A and C images are 2 μm, and for B and D images are 200 nm.

amine derivatives (such as ammonia-borane) with the use of Cu catalysts [44,45].

2. Experimental

Chemical reagents were purchased from Sigma–Aldrich in analytical grade.

Ultrapure water (electrical resistance of 18 MΩ) from an EasyPure RF (Barnstead) source was used throughout all the experiments.

The electrochemical experiments were conducted with the use of a PC-controller (Autolab GPES software, version 4.9) and Autolab potentiostat/galvanostat (PGSTAT302N). All measurements were performed in room-temperature.

Woven-copper electrodes, 99.5%, (wire thickness 150 μm, 10 mm wide and 1.5 mm thick) were purchased from Teknolabor.

Commercial air cathodes (type E4, MnO_2 catalyst) were purchased from Electric Fuel.

Electrochemical measurements were performed in a standard three-electrode cell, comprising a working electrode (consisting of the examined metal), high-surface-area carbon electrode (2 cm × 0.5 cm) as counter electrode and Ag/AgCl (sat. KCl) as reference electrode (Metrohm).

Full-cell measurements were performed in a homemade PVC device, 200 mL volume.

Nanostructured-copper electrodes were prepared in the following way [46]. A conventional 4 cm^2 woven-copper electrode was soaked for 30 min in 3 mL of a heated solution of 0.2 M $CuSO_4$ and 0.8 M ammonia. When the temperature reached 65 °C, 3 mL of 0.3 M NaH_2PO_2 (reducing agent) was added. The electrode was kept in this solution for 3 h at 65 °C. The electrode was then washed with pure water and ethanol and kept in acetonitrile before being used. The different woven-copper electrodes were imaged by HRSEM (Jeol, JSM-6700F).

The cathode protective layer [47] was prepared by coating the commercial air cathode (60 cm^2) by 2.5 mL of a solution containing 5% (w v^{-1}) poly(vinyl alcohol-co-ethylene) (ethylene content 27 mol%) and 5% (w v^{-1}) polyethylene glycol (average molecular weight 200) in n-propane and water (1:1, v v^{-1}) and dried at 120 °C for one hour.

Discharge-efficiency experiments were performed in various galvanostatic regimes and the efficiency of the discharge process was calculated according to Eq. (2)

$$\eta = Q_d Q_t^{-1} 100\% \quad (2)$$

where η is the efficiency (reported as a percentage), Q_t is the calculated theoretical charge (Coulombs, corresponding to the amount of hydrazine) and Q_d is the real charge derived from the discharge curves.

2.1. Roughness factor determination

Cyclic voltammograms were performed with the use of our different Cu electrodes, smooth and *nanostructured*, in non-faradic range (3 M NaOH, between −1.2 V and −0.7 V, 100 mV s^{-1}). The ratio between the ΔiP (A) at $E = -0.95$ V of the *nanostructured* Cu electrode and the smooth Cu electrode corresponds to the surface area ratio between both electrodes.

3. Results and discussion

The electrochemical properties of hydrazine in alkaline solution with the use of a copper catalyst were compared to the properties obtained with gold and silver catalysts (bare polished electrodes). The Cu/hydrazine anode produces the lowest OCP (−0.85 V), while

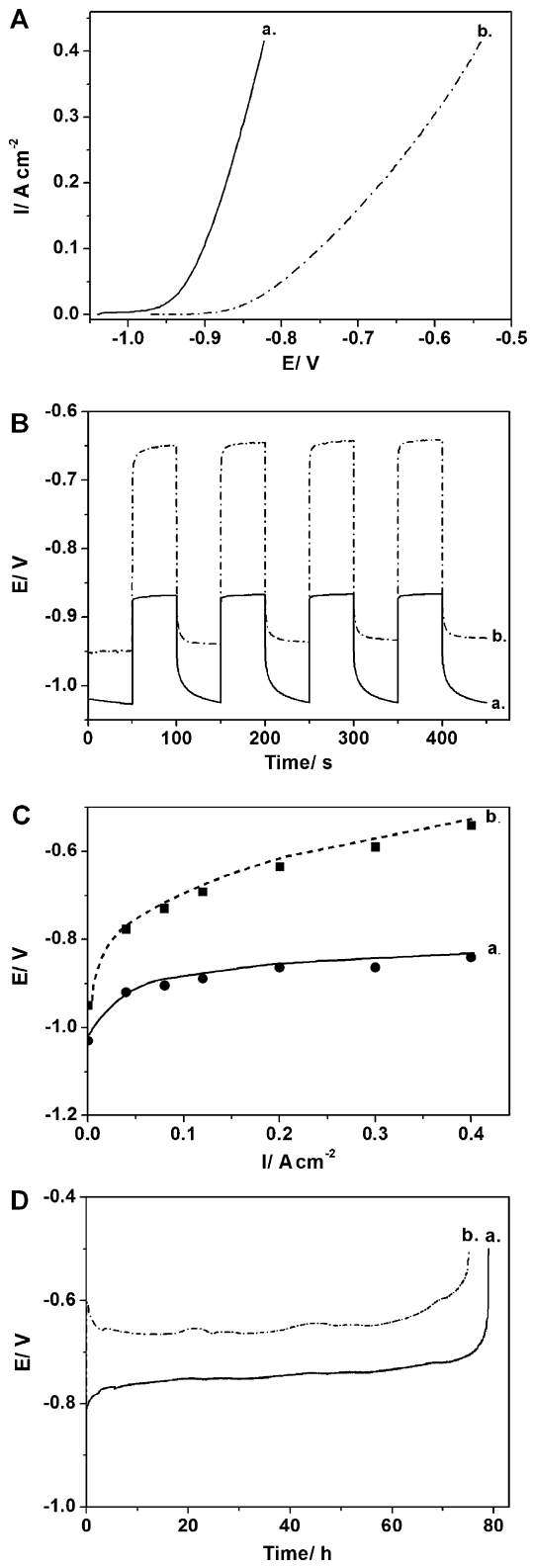

Fig. 3. (A) The electro-oxidation of hydrazine (20 mV s^{-1}) on different woven-Cu electrodes: (a) *nanostructured* and (b) conventional. (B): Typical transient measurements between 0 A (OCP condition) and 0.5 A (0.2 A cm^{-2}) with (a) *nanostructured* and (b) conventional woven-Cu electrodes. (C): Derived E vs. I curve, (a) *nanostructured* woven-Cu electrode and b) conventional woven-Cu electrode. (D): Extended full discharge at 0.5 A (0.2 A cm^{-2}) with the use of different type of (a) *nanostructured* and (b) conventional woven-Cu electrodes. In all experiments; 10 × 1-cm strips of woven-Cu were folded twice into 2.5 cm^2 rectangles. The solution (190 mL) contains 2.1 M (12.8 g) hydrazine, 9 M KOH. Ag/AgCl (sat. KCl) was used as the reference electrode.

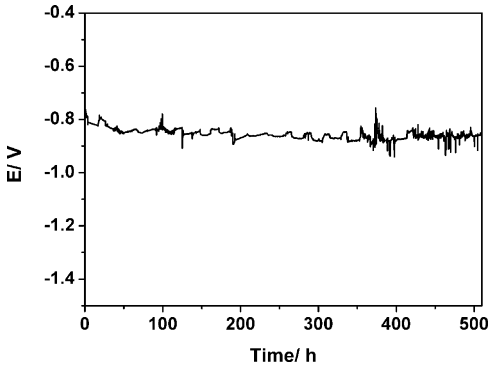

Fig. 4. Extended discharge at 0.5 A (0.2 A cm^{-2}) with the use of *nanostructured* Cu electrodes (as described in Fig. 3). The electrochemical experiment was started in 9.9 M hydrazine (14.3 g), 6 M KOH (45 mL solution). Every two days 20 mL solution was removed from the cell and 20 mL of 10.1 M hydrazine (6.5 g) in 6 M NaOH was added. Ag/AgCl (sat. KCl) was used as the reference electrode.

the Ag/hydrazine anode produces an OCP of −0.65 V (vs. Ag/AgCl), and the Au/hydrazine anode produces an OCP of −0.80 V.

A comparison of the oxidation currents generated by the three metal catalysts, in order to examine the intrinsic Cu catalyst activity, was performed. All three catalysts (geometrical area of 0.5 cm^2, 99.99%) show catalytic activity for the electro-oxidation of hydrazine. The oxidation current generated by the copper catalyst (Fig. 1, curve a) appears at an on-set potential above ca. −0.75 V, while the currents generated by the gold and silver catalysts appear at an on-set potential above ca. −0.65 V (curves b and c, respectively). In addition, the oxidation current generated by the copper catalyst is significantly higher than those observed for silver and gold electrodes of the same dimensions, in the potential range of −0.75 to −0.40 V. At $E = -0.50$ V, the current for copper is five times higher that for gold, while the silver catalyst generates a negligible oxidation current at this potential.

Similar results were also observed by Azazawa et al. [33], but no additional experiments using the copper catalyst were performed.

The negative shift of the on-set potential, 100 mV, between the Au/hydrazine and the Cu/hydrazine anodes (−0.65 V and −0.75 V, respectively), as well as the increased oxidation current generated by the Cu catalyst, clearly shows that the Cu catalyst is a prospective material for the electro-oxidation of hydrazine.

In order to increase the current density, we used large-area woven-copper electrodes, as well as *nanostructured* woven-copper electrodes. The *nanostructured* woven-copper electrodes were prepared by chemical treatment of the conventional woven-copper electrodes [46].

The *nanostructured* woven-copper electrodes were imaged by high-resolution scanning electron microscopy (HRSEM), as presented in Fig. 2A and B, compared with the conventional woven-copper electrodes, Fig. 2C and D. The *nanotextured* copper electrodes show high roughness, and are covered by closely packed copper particles in the size range of several micrometers (Fig. 2A). Closer inspection of these large-diameter particles reveals a clear *nanotextured* faceted appearance, each particle formed by numerous, sharp petal-like elements, with a thickness of 5–10 nm and nominal diameters ranging from 100 to 400 nm, similar to the structure of a "lotus-flower", (Fig. 2B). On the other hand, conventional woven-copper substrates show a smooth surface topography (Fig. 2C and D). The roughness factor between the *nanostructured* woven-Cu electrode and the smooth woven Cu-electrode corresponds to ca. 20. These striking differences between the untreated smooth substrates and the *nanotextured*-copper surfaces are expected to have a major influence on the electrochemical oxidation of hydrazine.

The electro-oxidation of hydrazine was carried out with the use of the *nanotextured* woven-copper electrode and with the conventional woven-copper electrode (geometrical area of 2.5 cm^2). The results are presented in Fig. 3A, curves a and b respectively. The oxidation current generated by the *nanotextured* woven-copper electrode (curve a) appears at a potential above about −0.95 V, while the corresponding potential for the conventional electrode is about −0.85 V (curve b). As a result, the oxidation current generated by the *nanotextured* electrode is significantly higher than that for the conventional electrode of equivalent geometrical area. The oxidation current generated by the *nanotextured* electrode at $E = -0.85$ V is about 20 times higher than the current observed for the conventional copper electrode of the same geometrical area.

Our *nanotextured* copper electrode produces two important characteristics: higher oxidation current due to increased surface area and an additional nano-catalytic effect, a negative shift of the on-set potential of about 100 mV (−0.85 V to −0.95 V), Fig. 3A. This negative shift is a clear evidence of the nano-Cu catalysis effect. To our knowledge, there have been no previous literature reports

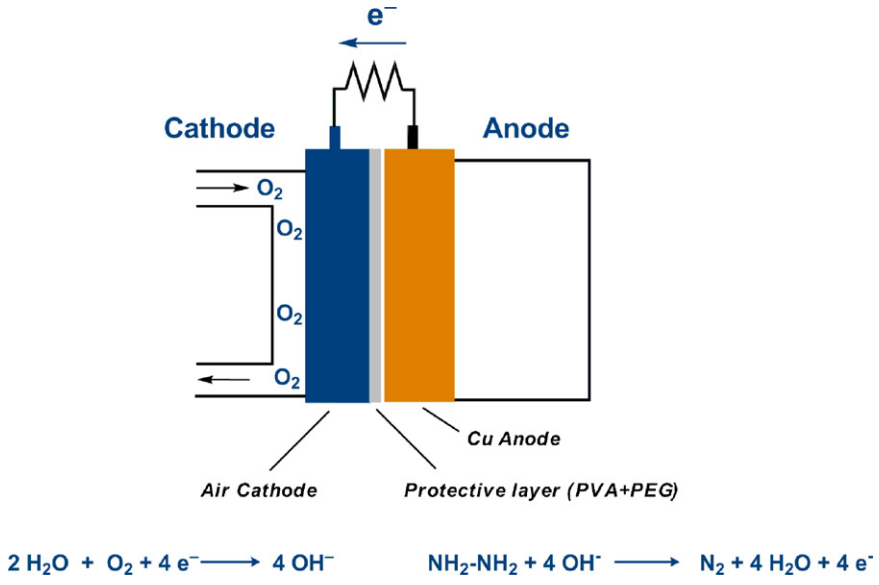

Fig. 5. General description of our hydrazine/air fuel cell.

showing this effect. The nature of this effect has not yet been clarified, and further investigation is required in this context. A plausible explanation could involve the increased amount of Cu(II) species on the nano-Cu surface, such as $Cu(OH)_2$, CuOOH and/or $Cu(N_2H_4)_n^{2+}$. These species function as catalysts for the electron-transfer process on the *nano*-Cu surface. As mentioned before, Cu^{2+} ion is a powerful catalyst for the decomposition of hydrazine and hydrazine derivatives. The reaction results in the reduction of Cu^{II} species to Cu^0. In addition, Cu can be oxidized in alkaline solution to Cu^{n+} species, and the equilibrium $Cu^0 \leftrightarrow Cu^{n+}$ is developed. In OCP regime (no oxidation current) the equilibrium depends on the hydrazine and hydroxide concentration. This effect is significantly increased on nano-Cu high-surface electrodes, since the surface area is significantly higher.

Under OCP (zero-current) conditions, the concentration of Cu^{n+} species on the copper surface is low ($[Cu^{n+}] \ll [Cu^0]$), since the concentration of hydrazine (a reducing agent) near the copper surface is high. When hydrazine is being electro-oxidized, its concentration on the copper surface decreases (a depletion layer is formed) and the concentration of Cu^{n+} species on the copper surface increases. Similar behavior has been observed recently [10–12]. These publications report on studies of the electro-oxidation of copper in alkaline media with the use of different techniques. According to these studies, five peaks can be assigned to three major single-electron processes involving Cu(0)/Cu(I), Cu(I)/Cu(II), and even unusual Cu(II)/Cu(III) transitions in the cyclic voltammogram of the copper electrode. These reports suggested the presence of CuO, Cu_2O and $Cu(OH)_2$ on the Cu surface, whereas in solution, the presence of some other species was postulated. It seems that the formation of a stable layer of copper (hydr)oxide on the surface of the copper electrode, in alkaline solution, can protect it from corrosion.

In the case of higher surface area (*nanostructured* Cu), the concentration of Cu^{n+} species on the copper surface is higher. The mechanism of catalysis includes self-management of Cu^{n+} species on the copper surface. In the discharge regime, the concentration of Cu^{n+} species increases (for the reasons mentioned above).Transient experiments between 0 A (OCP condition) and 0.5 A (0.2 A cm^{-2}) were also performed, and typical curves are shown in Fig. 3B for both types of the woven-copper electrode. The response time between OCP and 0.5 A is <0.1 s for both types of electrodes. The conventional woven-copper electrode produces an OCP of −0.95 V and a working potential of −0.65 V (vs. Ag/AgCl) at 0.5 A (0.2A cm^{-2}), while the *nanotextured* woven-copper electrode produces OCP of about −1.02 V and a working potential of about −0.87 V. This negative shift of the OCP values (between −0.95 V and −1.02 V is attributed to the nanocatalytic effect.

Fig. 3C presents the E vs. I curve for both types of woven-copper electrodes. The potential of the *nanostructured* electrode (curve a) is significantly more negative than that for the conventional electrode (curve b). Full discharge at 0.5 A (0.2 A cm^{-2}) for the two electrodes is shown in Fig. 3D. Relatively stable potentials were observed: about −0.68 V for the conventional electrode (curve a) and about −0.78 V for the *nanostructured* electrode (curve b). The *nanotextured* woven-copper/hydrazine anode shows lower oxidation overpotential compared to the smooth woven-copper/hydrazine anode (Fig. 3B–D). This phenomenon is attributed to the increased surface area of the *nanotextured* woven-copper electrode. The hydrazine discharge efficiency corresponds to about 90% in each case, thus four electrons are involved in the electro-oxidation process of hydrazine according to reaction (1).

In order to examine the stability of the *nanostructured* electrode, a long, full-discharge experiment was performed for a period of 500 h galvanostatically, at 0.5 A (0.2 A cm^{-2}), as shown in Fig. 4. A relatively stable potential of about −0.80 V was observed; the *nanostructured* electrode is remarkably stable after 500 h (21 days).

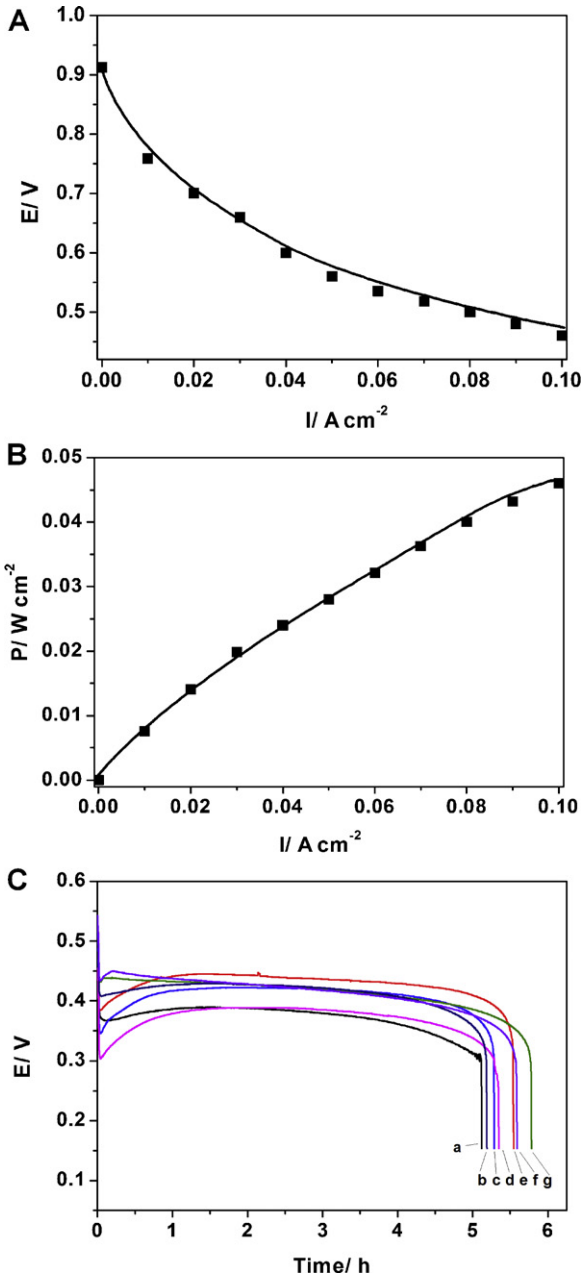

Fig. 6. (A) E vs. I (surface area corresponds to anode area) curve for our hydrazine/air fuel cell. (B) P vs. I curve. (C): Complete discharge at 1.0 A (0.1 A cm^{-2} corresponds to the anode area), (a) first cycle. (b)–(g) complete discharge cycles at 1.0 A (0.1 A cm^{-2} corresponds the anode area) upon hydrazine refueling (3 mL of 64% (0.3 M) hydrazine). The hydrazine/air fuel cell consists of 10 cm^2 *nanostructured* Cu anode and 24 cm^2 commercial air-cathode (platinum-free cathode). Anodic solution: 0.3 M hydrazine in 5.5 M KOH, 200 mL.

This observed stability is due to the fact that hydrazine is a good reducing agent for Cu(II) species (surface-formed Cu(II) species are reduced rapidly to Cu). No dissolution of copper was observed in all experiments and no mass losses for the electrodes were detected.

A fuel cell (200 mL volume) was constructed with a Cu/hydrazine anode, combined with a commercial air cathode coated by a protective layer of polyvinyl alcohol (PVA), and polyethylene glycol (PEG) [47], as shown in Fig. 5. Fig. 6A presents the E vs. I curve of the cell, and the derived P vs. I curve is shown in Fig. 6B. The OCP of our fuel cell is 0.92 V.

Seven full-discharge curves at 1 A (0.1 A cm^{-2} corresponds to the anode area) are shown in Fig. 6C. The output of the fuel cell is 0.45 W

at 1 A; it supplies 2.5 Wh and provides 1300 Wh kg^{-1} hydrazine. The hydrazine-discharge efficiency is about 85% (average of 20 discharge cycles). It should be emphasized that this hydrazine/air fuel cell does not require the addition of OH^- ion after the first cycle. Hydroxide ions are consumed in the anodic side (electro-oxidation of hydrazine) and formed in the cathodic side (electro-reduction of oxygen), and transferred back through the protective layer to the anodic side (Fig. 5).

Our Cu-hydrazine/air fuel cell properties were compared to a state-of-the art hydrazine/oxygen fuel cell based on the use of nano-Pt as anode and cathode catalysts, and pure oxygen as oxidant, as developed by Yamada et al. [32]. Yamada et al. Pt-hydrazine/oxygen fuel cell produces similar OCP of 0.92 V at a pure oxygen flow rate of 100 mL min^{-1}. Our fuel cell produces a similar OCP value with the use of air (not pure oxygen), and without the use of any air pump; the cathode consumes the oxygen directly from the air. Our Cu-hydrazine/air fuel cell supplies 0.4 V at 0.1 A cm^{-2}, while the Pt-hydrazine/oxygen fuel cell supplies this voltage only with the use of pure oxygen and oxygen pump. In addition, our non-noble metal Cu-hydrazine/air fuel cell is significantly simpler and of dramatically lower cost when compared to the Pt-hydrazine/oxygen fuel cell.

4. Conclusions

A new nanostructured-Cu/hydrazine anode has been developed, which is characterized by high catalytic activity as compared to Au/hydrazine, Ag/hydrazine and Pt/hydrazine anodes. This nano-Cu/hydrazine anode shows discharge characteristics superior to those of platinum and platinum-group-metal catalysts. It is highly stable for more than 500 h at a discharge current of 0.5 A (0.2 A cm^{-2}). The hydrazine/air fuel cell, in which this anode was applied, shows a power output of about 0.45 W at 1 A (the anode area corresponds to 0.1 A cm^{-2}) and a discharge efficiency for hydrazine of about 85%.

This novel Cu/hydrazine anode can be widely used in high-power fuel-cell applications (e.g. vehicle engines). Its components are simple and low-cost, and the by-products of its operation (nitrogen and water) are non-polluting.

Acknowledgement

We acknowledge Nanergy Ltd for the financial support.

References

[1] G.H. Miley, N. Luoa, J. Mather, R. Burton, G. Hawkins, L. Gua, E. Byrd, R. Gimlin, P.J. Shrestha, G. Benavides, J. Laystrom, D. Carroll, J. Power Sources 165 (2007) 509–516.
[2] N.Q. Minh, J. Am. Ceram. Soc. 76 (1993) 563–588.
[3] T.E. Springer, T.A. Zawodzinski, S. Gottesfeld, J. Electrochem. Soc. 138 (1991) 2334–2342.
[4] L. Carrette, K.A. Friedrich, U. Stimming, ChemPhysChem 1 (2000) 162–193.
[5] R. Parsons, T. Vandernoot, J. Electroanal. Chem. 257 (1988) 9–45.
[6] O. Yamamoto, Electrochim. Acta 45 (2000) 2423–2435.
[7] U.B. Demirci, J. Power Sources 169 (2007) 239–246.
[8] V. Mehta, J.S. Cooper, J. Power Sources 114 (2003) 32–53.
[9] S.P. Jiang, Mater. Sci. Eng. A418 (2006) 199–210.
[10] G. Karim-Nezhad, R. Jafarloo, P.S. Dorraji, Electrochim. Acta 54 (2009) 5721–5726.
[11] J. Kunze, V. Maurice, L.H Klein, H.-H. Strehblow, P. Marcus, J. Electroanal. Chem. 113–125 (2003) 554–555.
[12] J. Kunze, V. Maurice, L.H. Klein, H.-H. Strehblow, P. Marcus, J. Phys. Chem. B 105 (2001) 4263–4269.
[13] S. Wasmus, A. Kuver, J. Electroanal. Chem. 461 (1999) 13–14.
[14] X.M. Ren, P. Zelenay, S. Thomas, J. Davey, S. Gottesfeld, J. Power Sources 86 (2000) 111–116.
[15] H. Liu, C. Song, L. Zhang, J. Zhang, H. Wang, D.P. Wilkinson, J. Power Sources 155 (2006) 95–110.
[16] S.C. Amendola, P. Onnerud, M.T. Kelly, P.J. Petillo, S.L. Sharp-Goldman, M. Binder, J. Power Sources 84 (1999) 130–133.
[17] Pletcher, D.J. Browning, J.B. Lakemanc, J. Power Sources 155 (2006) 172–181.
[18] C.P.D. León, F.C. Walsh, A. Rose, J.B. Lakemana, D.J. Browning, R.W. Reeve, J. Power Sources 164 (2007) 441–448.
[19] R.K. Raman, A.K. Shukla, Fuel Cells 3 (2007) 225–231.
[20] J.H. Wee, J. Power Sources 155 (2006) 329–339.
[21] N.A. Choudhurya, R.K. Ramana, S. Sampathb, A.K. Shukla, J. Power Sources 143 (2005) 1–7.
[22] U.B. Demirci, P. Miele, Energ. Environ. Sci. 2 (2009) 627–637.
[23] X.B. Zhang, S. Han, J.M. Yan, H. Shioyama, N. Kuriyama, T. Kobayashi, Q. Xu, Int. J. Hydrogen Energ. 34 (2009) 174–179.
[24] C. Yao, H. Yang, L. Zhuang, X. Ai, Y. Cao, J. Lu, J. Power Sources 165 (2007) 125–127.
[25] X.B. Zhang, S. Han, J.M. Yan, M. Chandra, H. Shioyama, K. Yasuda, N. Kuriyama, T. Kobayashi, Q. Xu, J. Power Sources 168 (2007) 167–171.
[26] X.B. Zhang, J.M. Yan, S. Han, H. Shioyama, K. Yasuda, C.N. Kuriyama, Q. Xu, J. Power Sources 182 (2008) 515–519.
[27] A. Serov, C. Kwak, Appl. Catal. B-Environ. 98 (2010) 1–9.
[28] A. Upton, N. Johnson, J. Sandy, E. Sim, Trends Pharmacol. Sci. 22 (2001) 140–146.
[29] G. Evans, K. Kordesch, Science 158 (1967) 1148–1152.
[30] S.J. Laoa, H.Y. Qina, L.Q. Yea, B.H. Liub, Z.P. Li, J. Power Sources 195 (2010) 4135–4138.
[31] K. Yamada, K. Yasuda, H. Tanaka, Y. Miyazaki, T. Kobayashi, J. Power Sources 122 (2003) 132–137.
[32] K. Yamada, K. Asazawa, K. Yasuda, T. Ioroi, H. Tanaka, Y. Miyazaki, T. Kobayashi, J. Power Sources 115 (2003) 236–242.
[33] K. Asazawa, T. Sakamoto, S. Yamaguchi, K. Yamada, H. Fujikawa, H. Tanaka, K. Oguro, J. Electrochem. Soc. 156 (2009) B509–B512.
[34] K. Asazawa, K. Yamada, H. Tanaka, A. Oka, M. Taniguchi, T. Kobayashi, Angew. Chem. Int. Ed. 46 (2007) 8024–8027.
[35] Q. Yi, L. Li, W. Yu, Z. Zhou, G. Xu, J. Mol. Catal. A-Chem. 295 (2008) 34–38.
[36] M. Michlmatr, D.T. Sawyer, J. Electroanal. Chem. 23 (1969) 375–385.
[37] K. Asazawa, K. Yamada, H. Tanaka, M. Taniguchi, K. Oguro, J. Power Sources 191 (2009) 362–365.
[38] L.Q. Ye, Z.O. Li, H.Y. Qin, J.K. Zhu, B.H. Liu, J. Power Sources 196 (2011) 956–961.
[39] A. Abbaspour, M.A. Kamyabi, J. Electroanal. Chem. 576 (2005) 73–83.
[40] Y.D. Zhao, W.D. Zhang, H. Chen, Q.M. Luo, Talanta 58 (2002) 529–534.
[41] Z. Jiang, X. Liao, A. Deng, A. Liang, J. Li, H. Pan, J. Li, S. Wang, Y. Huang, Anal. Chem. 80 (2008) 8681–8687.
[42] C.R. Wellman, J. Ward, L.P. Kuhn, J. Am. Chem. Soc. 98 (1976) 1683–1684.
[43] X. Lin, Q. Pan, G. Rempel, Appl. Catal. A-Gen. 263 (2004) 27–32.
[44] F. Patolsky, B. Filanovsky, E. Granot, PA WO/2010/055511.
[45] B. Filanovsky, E. Granot, R. Dirawi, I. Presman, I. Kuras, F. Patolsky, Nano Lett. 11 (2011) 1727–1732.
[46] J.G. Yang, S.H. Yang, C.B. Tang, H.E Jing, M.T. Tang, Trans. Nonfer. Met. Soc. China 12 (2007) s1181–s1185.
[47] B. Smith, S. Sridhar, A.A. Khan, J. Membrane Sci. 259 (2005) 10–26.